JMEPEG (2009) 18:1116–1123
DOI: 10.1007/s11665-008-9335-0

1059-9495/$19.00

Effect of Heat Input on Microstructural Changes and Corrosion Behavior of Commercially Pure Titanium Welds in Nitric Acid Medium

A. Ravi Shankar, G. Gopalakrishnan, V. Balusamy, and U. Kamachi Mudali

(Submitted March 4, 2008; in revised form October 21, 2008)

Commercially pure titanium (Ti) has been selected for the fabrication of dissolver for the proposed fast reactor fuel reprocessing plant at Kalpakkam, India. In the present investigation, microstructural changes and corrosion behavior of tungsten inert gas (TIG) welds of Ti grade-1 and grade-2 with different heat inputs were carried out. A wider heat affected zone was observed with higher heat inputs and coarse grains were observed from base metal toward the weld zone with increasing heat input. Fine and more equiaxed prior β grains were observed at lower heat input and the grain size increased toward fusion zone. The results indicated that Ti grade-1 and grade-2 with different heat inputs and different microstructures were insensitive to corrosion in liquid, vapor, and condensate phases of 11.5 M nitric acid tested up to 240 h. The corrosion rate in boiling liquid phase (0.60-0.76 mm/year) was higher than that in vapor (0.012-0.039 mm/year) and condensate phases (0.04-0.12 mm/year) of nitric acid for Ti grade-1 and grade-2, as well as for base metal for all heat inputs. Potentiodynamic polarization experiment carried out at room temperature indicated higher current densities and better passivation in 11.5 M nitric acid. SEM examination of Ti grade-1 welds for all heat inputs exposed to liquid phase after 240 h showed corrosion attack on the surface, exposing Widmanstatten microstructure containing acicular alpha. The continuous dissolution of the liquid-exposed samples was attributed to the heterogeneous microstructure and non-protective passive film formation.

Keywords corrosion testing, joining, titanium

1. Introduction

Corrosion-resistant materials like titanium and zirconium are candidate materials in fast reactor reprocessing plants for fabricating components like dissolver and evaporator, where high concentration of nitric acid and high temperatures are involved (Ref 1, 2). For the reprocessing of fast reactor carbide fuel from fast breeder test reactor (FBTR), at Kalpakkam, India, unalloyed grade-2 titanium has been used in the construction of dissolver. For the proposed demonstration fast reactor fuel reprocessing plant (DFRP), Ti has been selected for the fabrication of dissolver.

For the fabrication of reactive materials like titanium and zirconium dissolver, gas-tungsten arc (TIG) welding is extensively used. During onsite welding of some of the components, difficulties were experienced in controlling the heat input. Heat input depends on applied variables like voltage, current, and travel speed. Travel speed affects the width and penetration of a TIG weld, so other variables like current and voltage have to be adjusted for constant heat input. Heat input can be calculated by the following equation. Heat input (J/mm) = (voltage (V) × current (A))/travel speed (mm/min). Heat input affects the microstructure and hence the microstructure-sensitive properties of the weld metal.

Commercially pure titanium has good corrosion resistance in boiling 11.5 M nitric acid medium in contrast to austenitic stainless steels (Ref 1-3). Ti-based alloys such as Ti-5Ta (Ref 3, 4), Ti-5Ta-1.8Nb (Ref 4, 5) have shown better corrosion resistance than Ti. The weldability of new developmental Ti-5Ta-1.8Nb alloy was also excellent (Ref 6); however, corrosion behavior of titanium welds with different heat inputs was not known.

In the present investigation, comparative studies of microstructural changes and corrosion behavior of Ti grade-1 and grade-2 TIG welds were done in a corrosion medium of boiling 11.5 M nitric acid with different heat inputs.

2. Experimental Details

2.1 Materials

The nominal chemical composition of Ti grade-1 and grade-2 used for TIG welding are given in Table 1. The mechanical properties of titanium grade-1 and grade-2 used are given in Table 2. Titanium grade-1 and grade-2 plates of 35 mm width × 100 mm length and 6 mm thickness with suitable

A. Ravi Shankar and **U. Kamachi Mudali**, Corrosion Science and Technology Division, Indira Gandhi Centre for Atomic Research, Kalpakkam 603 102, India; and **G. Gopalakrishnan** and **V. Balusamy**, Department of Metallurgical Engineering, P.S.G. College of Technology, Coimbatore, India. Contact e-mail: kamachi@igcar.gov.in.

Table 1 Nominal chemical composition (wt.%) of Ti grade-1 and grade-2 plates used for TIG welding

S. no.	Material	C	Fe	H	O	N	Ti
1	Grade-1	0.19	0.2	0.15	0.148	0.017	Bal
2	Grade-2	0.19	0.2	0.032	0.148	0.017	Bal

Table 2 Mechanical properties of Ti grade-1 and grade-2 plates used for TIG welding

S. no.	Material	0.2% YS, MPa	UTS, MPa	Elongation, %	% RA
1	Grade-1	368	442	34	54
2	Grade-2	368	442	34	54

v-groove preparation were used for TIG welding. The welded Ti grade-1 and grade-2 weld specimens were cut to desired dimensions and polished up to 600 grit emery paper for three-phase corrosion test, while for polarization studies the samples were mounted and polished up to 1200 grit emery paper.

2.2 TIG Welding Process

Gas-tungsten arc welding (TIG) is used extensively for welding stainless steel, copper, and reactive materials like titanium, tantalum, etc. Welding of reactive materials requires that contamination level be less than 50 ppm, which necessitates the use of gas purifiers or ultra purity argon as shielding gas (Ref 7). Depending on the severity of contamination, the color of weld bead and heat affected zone (HAZ) may vary from light straw to dark blue or grey. Welds that are dark blue or grey have to be totally rejected (Ref 8). The fabrication of welds was carried out at M/s. Ti Anode Equipment Limited, Chennai. TIG welding process was carried out with shielding gas (high-purity argon) being fed through the torch to protect the electrode, molten weld pool, and solidifying weld metal from contamination by the atmosphere. Apart from this, trailer inert gas shielding and back shielding was also provided. Heat input was varied primarily by varying the travel speed. The average heat input of titanium grade-1 and grade-2 TIG welds are tabulated in Table 3. The welded plates were subjected to radiographic examination using SEIFERT 200 MFI equipment and microhardness measurements were made along the welds.

2.3 Three-Phase Corrosion Test

Three-phase corrosion test was carried out on Ti grade-1 and grade-2 base as well as on welds with different heat inputs in boiling 11.5 M nitric acid. The test was carried out for 48 h and weight losses were recorded and the corrosion rates were calculated. The test was repeated for five such 48 h periods and average corrosion rates were calculated. The details of the three-phase corrosion test and experimental set up are described elsewhere (Ref 4, 5).

2.4 Polarization Studies

The potentiodynamic polarization studies were carried out in 11.5 M nitric acid at room temperature. The sample was held at open circuit potential for 30 min and polarization was carried out at a scan speed of 10 mV/min. The reference electrode used was saturated calomel electrode (SCE) and tests were carried out from 200 mV below the open circuit potential to a potential of +2200 mV versus SCE.

Table 3 Average heat input (J/mm) of Ti grade-1 and grade-2 TIG welds

S. no.	Titanium grade-1	Titanium grade-2
H1	1208	1025
H2	2255	3022
H3	3017	2466
H4	1752	1622

2.5 Microstructural Characterization and Surface Morphology

The welded samples were polished to mirror finish using alumina paste and etching was done using 5 mL HF + 10 mL HNO_3 + 85 mL distilled water as etchant. The effect of heat input on the microstructure was studied using optical microscope. The surface morphology of the corroded samples was examined using Philips XL-30 scanning electron microscope.

2.6 Profilometry

Profilometry measurements were carried out in order to observe the changes in surface roughness and preferential attack of weldment with respect to base metal. Profilometry for Ti grade-2 in etched and corroded condition was carried out for heat input 3 and 4 weldment in corroded condition using a DEKTAK-3 surface profilometer.

3. Results and Discussion

3.1 Radiography

The radiographic examination carried out on manual TIG welded Ti grade-1 and grade-2 plates was found to be acceptable as per ASME section III acceptance criterion. However, the radiography results clearly indicated 0.5 mm ∅ porosity in the plates welded at higher heat input. This clearly shows that higher heat input results in poor quality welds.

3.2 Microstructure

The two types of alpha phase present in Ti alloys are primary alpha and secondary alpha or transformed beta. The primary alpha is that present during prior hot working, remnants of which persist through heat treatment. The secondary alpha is produced by transformation from beta upon cooling from above the beta transus and appears in different morphologies known as acicular or lamellar, platelike, serrated, or Widmanstatten (Ref 9). The alpha that forms from beta is invariably acicular but with different degrees of fineness (Ref 10). Non-equilibrium martensite phases are produced as a function of alloy chemistry and processing and have an acicular structure and are difficult to differentiate from acicular alpha (Ref 10). The microstructures of base metal for Ti grade-1 and grade-2 are shown in Fig. 1(a) and (b), respectively. The microstructure consists of equiaxed α grain structure with fine precipitates present both within the grains and at grain boundaries.

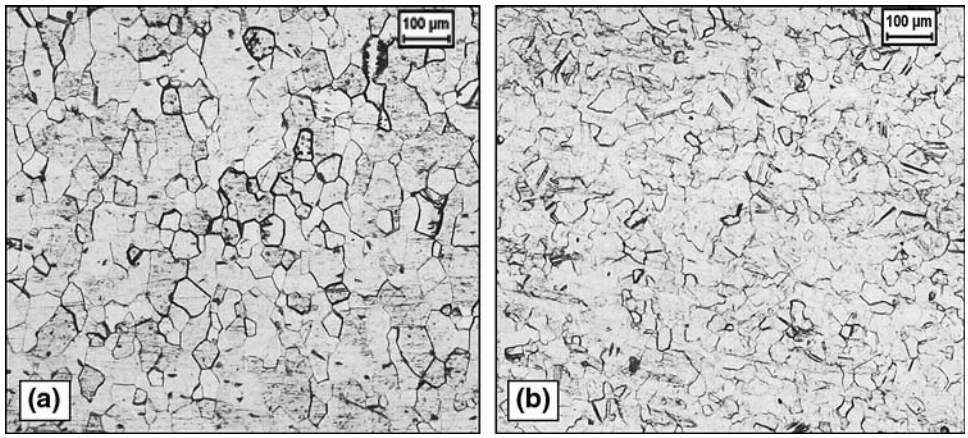

Fig. 1 Optical microstructure of the base metal of Ti (a) grade-1 and (b) grade-2

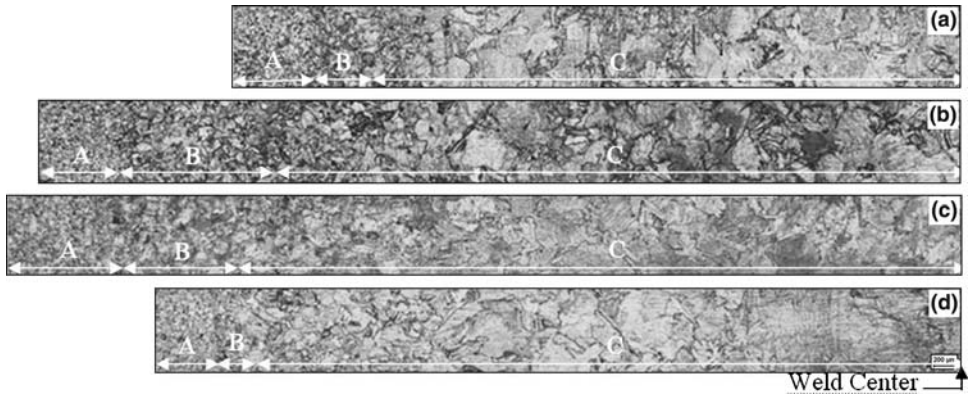

Fig. 2 Optical microstructure of the Ti grade-1 weld metal with heat input (a) H1, (b) H2, (c) H3, and (d) H4. A, base metal; B, HAZ; C, weld metal

During welding, the weld material is heated to a molten state and upon cooling the weld will exhibit a transformed grain structure or acicular α grains surrounded by prior β grain boundaries (Widmanstatten or basketweave structure). The size and shape of prior β grains and the transformations that take place during solidification are important characteristics (Ref 11). The microstructural sensitivity with high heat input and rapid cooling of advanced titanium alloys is related to the weldability problems and the affected microstructures suffer from poor ductility and toughness (Ref 12). The fusion zone beta grain size depends primarily on the weld energy input, with a higher energy input promoting a larger grain size and appreciable beta grain growth occurring in the near HAZ directly adjacent to the weld fusion zone (Ref 11). The microstructure for Ti grade-1 weldments with different heat inputs is shown in Fig. 2. Similar microstructure was obtained for Ti grade-2 weldments with different heat inputs. With respect to the heat inputs, the weld zone was wider for higher heat inputs for both Ti grade-1 and grade-2 compared to that for lower heat inputs. The variation in microstructure from base metal toward the weld zone with significant grain coarsening immediately adjacent to the HAZ is shown in Fig. 2. The degree of grain coarsening increases further toward the center of the fusion zone. In gas tungsten arc welding, as cooling rates decreases, with higher heat input (lower travel speed), there is an increasing amount of grain growth in the weld region promoting a larger grain size and a wider weld region. The higher cooling rate experienced with lower heat input promotes transformation of beta to fine, acicular, alpha/alpha prime microstructure.

The HAZ microstructure consists of primary alpha phase originating from the base-metal microstructure in a matrix of transformed beta (Ref 11). The HAZ adjacent to the base metal showed primary alpha and fine acicular structure compared to the base metal. From the weld microstructure it is clear that the prior β grains in the fusion zone are significantly coarser than the equiaxed grains in the base material and HAZ and the grain size increasing toward the fusion zone. The lower heat input produces finer, acicular alpha/alpha prime in the HAZ and smaller prior β grains compared to higher heat input. Both HAZ and fusion zone microstructures show the presence of acicular α formed by nucleation and growth within each prior β grain. In case of higher heat input, the width of HAZ and weld zone increases as compared to that of the lower heat input as evident from the microstructure shown in Fig. 2.

Table 4 shows the microhardness results of Ti grade-1 (H1) and grade-2 (H3) with different heat inputs. From Table 4 it is clear that there is only a marginal increase in hardness from base metal (145-164) to HAZ (161-172) to weld region (191-198). Even with different heat inputs, there is no noticeable change in hardness value.

3.3 Three-Phase Corrosion

Titanium weldments and associated HAZs generally do not experience corrosion limitations in welded components when normal passive conditions prevail for the base metal (Ref 13). However, for good mechanical properties and corrosion resistance, refinement of the prior β grain size is a requirement (Ref 14). Low heat input and slower welding speed have resulted in a greater proportion of the desirable fine, equiaxed, prior β grain structure and, in addition, lower heat input also reduced the width of the HAZ (Ref 14).

The average corrosion rate values for five individual periods in liquid, vapor, and condensate phases for Ti grade-1 and grade-2 with different heat input are tabulated in Table 5 and 6, respectively. The average corrosion rates for Ti grade-1 and grade-2 with different heat inputs were not much different in all the three phases, indicating that the corrosion rate was insensitive to heat input. The average corrosion rates for the welds were also not much different from the base metal in all three phases of 11.5 M nitric acid.

The average corrosion rate for Ti grade-1 and grade-2 base metal and welds with four different heat inputs in liquid phase was around 0.60-0.76 mm/year, in vapor phase, it was 0.012-0.039 mm/year, and in the condensate phase it was 0.04-0.12 mm/year. The lower corrosion rate in both vapor and condensate phases, while the higher dissolution in liquid phase, can be attributed to the formation of protective passive film in the condensate and vapor phases and the absence of passive film formation in liquid-exposed sample. The higher corrosion rate for the liquid-exposed samples may also be due to the presence of iron as impurity, resulting in higher dissolution. It is reported that at iron content above 0.05%, preferential corrosive attack of weld metal can occur in nitric acid because of the acicular nature of any retained beta phase that is stabilized by iron (Ref 11). The presence of 0.2% Fe in Ti grade-1 and grade-2 might have resulted in higher corrosion rates of around 0.762 mm/year in liquid phase; however, no preferential weld attack was observed in our study.

The corrosion rate in individual periods in liquid, vapor, and condensate phases of boiling 11.5 M nitric acid for Ti grade-1 and grade-2 with different heat input is shown graphically in Fig. 3(a)-(f). The individual corrosion rate for liquid-exposed samples of Ti grade-2 starts from a higher value compared to that of Ti grade-1 and also maximum corrosion rates were noticed in Ti grade-2 as shown in Fig. 3(e) and (f), indicating that grade-2 exhibits higher corrosion rate than grade-1.

Table 4 Average hardness of Ti with different heat input in different regions

Grade/heat input	Base	Base/weld interface	Weld zone	Base/weld interface	Base
Ti grade-1/1208 J/mm	145	164	198	161	147
Ti grade-2/2466 J/mm	164	172	191	169	163

3.4 Surface Morphology

The surface appearance of Ti weldments exposed to liquid phase was light yellow after 48 h and the weld microstructure was delineated; however, after 240 h of exposure, dark bluish color was observed. The SEM examination of the corroded samples exposed to 11.5 M boiling nitric acid for 240 h also revealed microstructure with uniform dissolution. SEM microstructure of the base metal of Ti grade-1 in boiling 11.5 M nitric acid for 240 h is shown in Fig. 4. Figure 4(a) shows the surface morphology of Ti grade-1 base metal with equiaxed alpha grains, and in some regions at higher magnification selective dissolution along grain boundaries was observed as shown in Fig. 4(b). It is reported that the segregated impurity elements in titanium such as iron dissolve in nitric acid and make titanium prone to hydrogen attack (Ref 3). SEM micrographs of Ti grade-1 (H3) exposed to vapor and condensate phases of 11.5 M nitric acid for 240 h are shown in Fig. 5(a) and (b), respectively. The surface morphology shows only minor attack in agreement with the corrosion rate values. Figure 6(a)-(f) shows SEM micrograph of base/weld interface, and weld zone for Ti grade-1. The weld microstructure with transformed β containing acicular α within prior β grain is shown. The base/weld interface consisting of primary alpha phase in a matrix of transformed beta for lower and higher heat input is shown in Fig. 6(a) and (b), respectively. The fine acicular alpha with small prior beta grain boundaries in the HAZ is shown in Fig. 6(e). The weld region consisting of acicular alpha with coarse prior beta grain boundary for lower and higher heat input is shown in Fig. 6(b) and (f), respectively. The acicular alpha and prior beta grains are comparatively coarser for higher heat input. Figure 6(c) shows the corrosion along acicular alpha in the weld region.

3.5 Potentiodynamic Polarization

The potentiodynamic anodic polarization curves for Ti grade-1 and grade-2 in 11.5 M nitric acid for base metal and welds with different heat inputs are shown in Fig. 7(a) and (b), respectively. The potentiodynamic anodic polarization of Ti grade-1 and grade-2 for base metal and welds with different heat inputs indicates good passivation; however, higher current densities were observed similar to higher corrosion rates in the

Table 5 Average corrosion rates (mm/year) of Ti grade-1 with different heat input in boiling 11.5 M nitric acid for 240 h

S. no.	Heat input	Liquid	Vapor	Condensate
1	BASE	0.622	0.030	0.073
2	H1	0.677	0.019	0.031
3	H2	0.682	0.012	0.019
4	H3	0.600	0.038	0.054
5	H4	0.520	0.039	0.046

Table 6 Average corrosion rates (mm/year) of Ti grade-2 with different heat input in boiling 11.5 M nitric acid for 240 h

S. no.	Heat input	Liquid	Vapor	Condensate
1	BASE	0.750	0.013	0.069
2	H1	0.639	0.021	0.097
3	H2	0.650	0.013	0.120
4	H3	0.744	0.032	0.068
5	H4	0.772	0.015	0.085

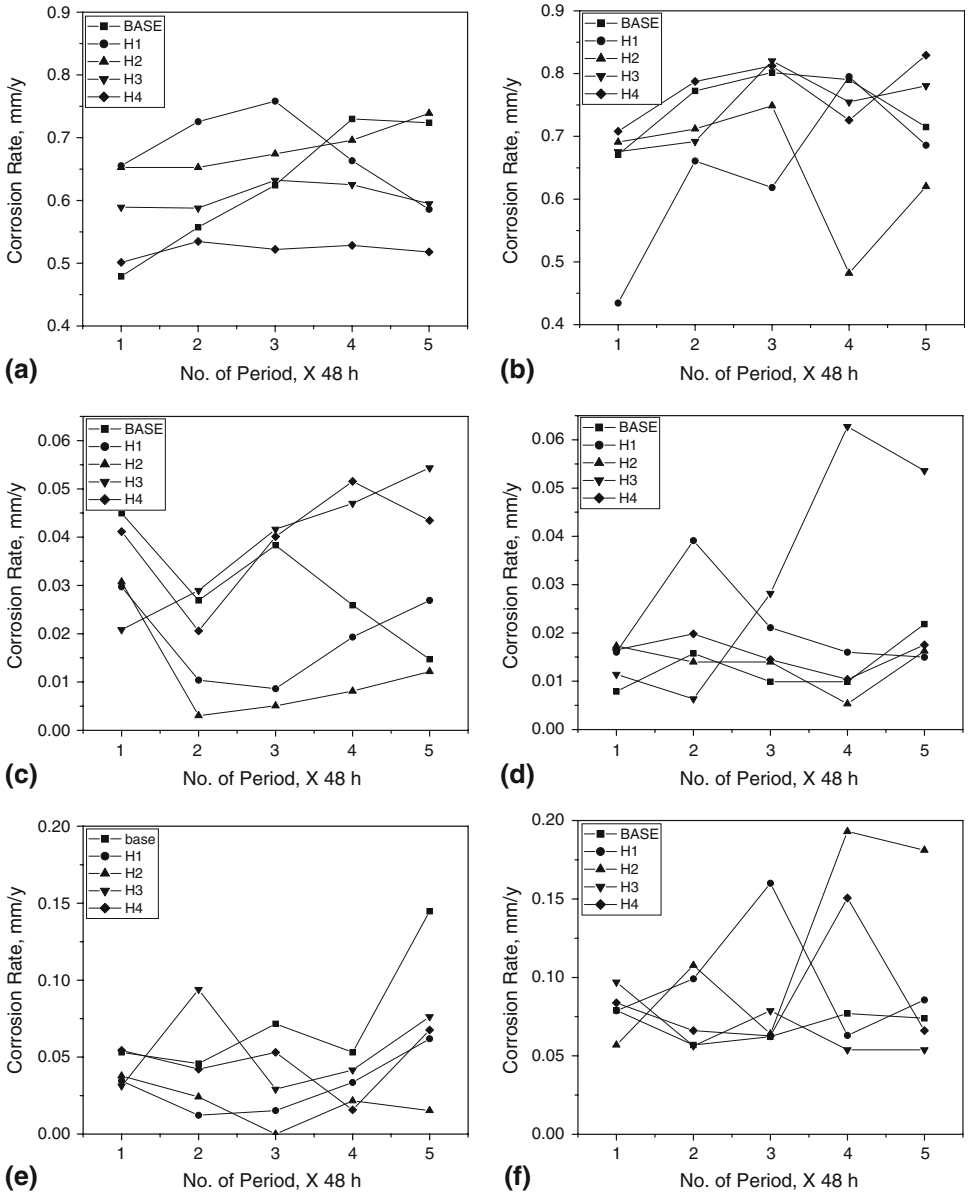

Fig. 3 Corrosion rate in 11.5 M nitric acid for Ti grade-1 in (a) liquid, (c) vapor, and (e) condensate phase, (b), (d), and (f) are for Ti grade-2 in liquid, vapor, and condensate phases, respectively

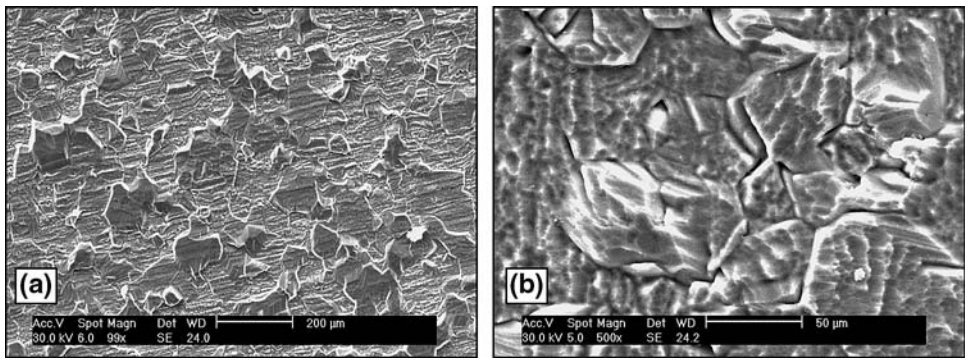

Fig. 4 SEM microstructure of the base metal of Ti grade-1 in boiling 11.5 M nitric acid for 240 h, exhibiting (a) uniform corrosion and (b) selective dissolution

three-phase corrosion test. Higher heat inputs result in poor weld quality, large HAZ/fusion zone, and consequently large heterogeneity in microstructure which might result in poor corrosion resistance over prolonged exposure.

3.6 Profilometry

Profilometry from the etched and corroded weldments clearly indicated increase in surface roughness of the corroded

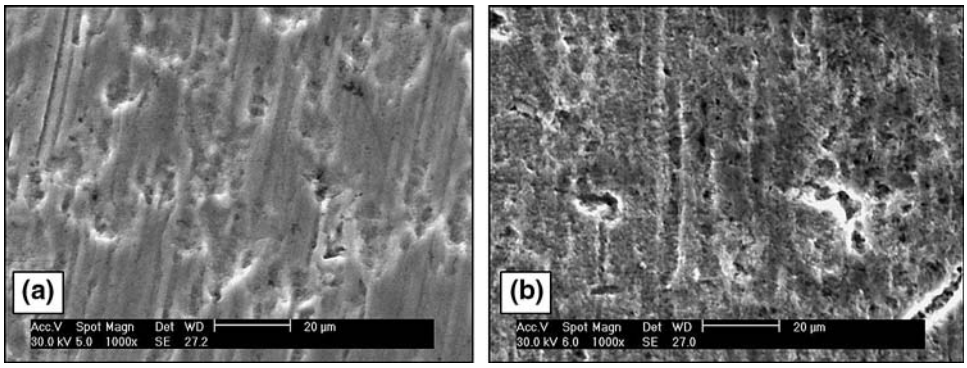

Fig. 5 SEM micrograph of Ti grade-1 (H3) exposed to (a) vapor and (b) condensate phases of 11.5 M nitric acid for 240 h

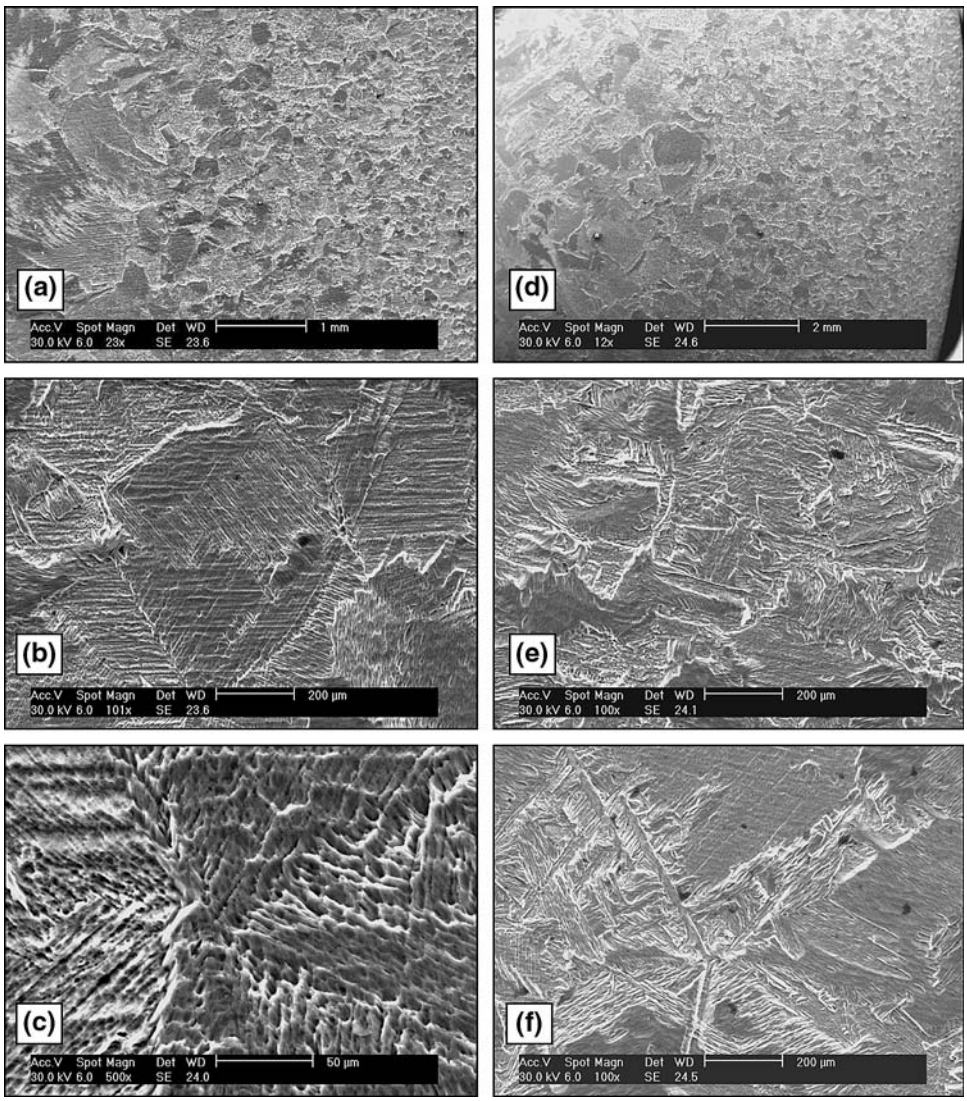

Fig. 6 SEM micrograph of Ti grade-1 exposed to liquid phase of 11.5 M nitric acid for 240 h for heat input H1 from (a) interface (b, c) weld region and for heat input H2 from (d) interface, (e) HAZ, and (f) weld region

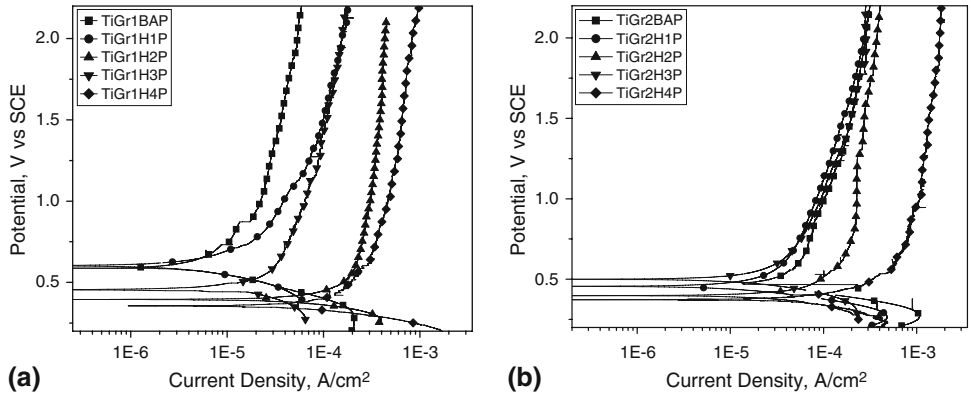

Fig. 7 Potentiodynamic anodic polarization curves for (a) Ti grade-1 and (b) Ti grade-2, with different heat inputs in 11.5 M nitric acid at room temperature

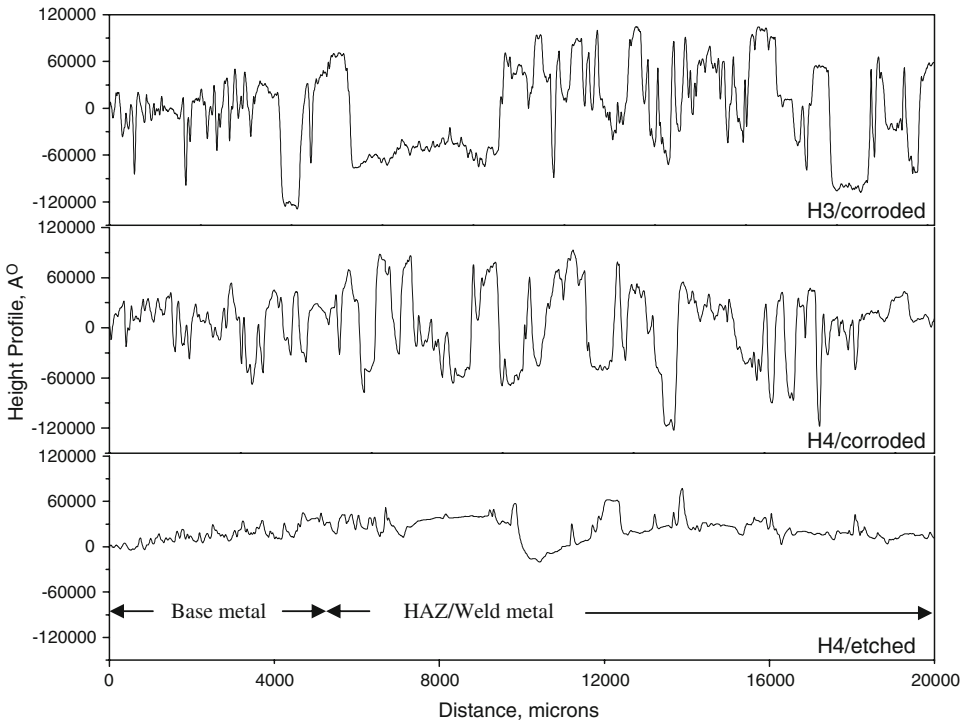

Fig. 8 Profilometry for Ti grade-2, heat input-4 weldment in etched and corroded condition and for heat input-3 weldment in corroded condition

samples in comparison to the etched sample. The spacing of the peaks in the base metal was less as compared to the HAZ/weld metal for the etched and corroded samples. This is due to corrosion along the interface of grain boundaries, with fine grain structure in the base metal and coarse prior beta grains in the weld region. Profilometry results in the etched and corroded condition of heat input 3 and 4 do not reveal any accelerated preferential corrosion attack in the weld region. The changes in surface roughness correspond to the uniform corrosion attack, while changes in the spacing of peaks correspond to the changes in grain size (Fig. 8).

4. Conclusions

1. The microstructure of Ti grade-1 and grade-2 from the base metal of TIG welded sample showed equiaxed α grain. A wider HAZ was seen for higher heat inputs and grain coarsening has occurred from base to the weld zone with increasing heat input. The lower heat input produces fine acicular alpha and prior β grains.
2. The corrosion rates of Ti grade-1 and grade-2 in boiling liquid, vapor, and condensate phases of 11.5 M nitric acid was not much different for base metal and welds with various heat inputs.
3. The corrosion rate in boiling liquid phase was higher than that in vapor and condensate phases of nitric acid, for Ti grade-1 and grade-2 base metal as well as for all heat inputs. The higher corrosion rate in the boiling liquid phase might be due to the presence of iron as impurity, which results in the formation of a non-protective film on the surface.
4. The SEM micrograph of Ti grade-1 liquid-exposed samples after 240 h of corrosion in 11.5 M nitric acid

revealed the microstructure changes. SEM micrographs of the samples with different heat input revealed the uniform dissolution of the Widmanstatten structure. The continuous dissolution of the liquid-exposed samples was evident, while the vapor and condensate exposed samples exhibited less corrosion attack which is in agreement with the corrosion rate data.

5. Potentiodynamic anodic polarization revealed good passivation properties for different heat input as well as for base metal in 11.5 M nitric acid at room temperature for both grades 1 and 2; however, higher current densities were observed.
6. Profilometry results from etched and corroded samples did not reveal any preferential corrosion at weld region.

References

1. B. Raj and U. Kamachi Mudali, Materials Development and Corrosion Problems in Nuclear Fuel Reprocessing Plants, *Prog. Nucl. Energy*, 2006, **48**, p 283–313
2. B. Raj, U. Kamachi Mudali, T. Jayakumar, K.V. Kasiviswanathan, and R. Natarajan, Meeting the Challenges Related to Material Issues in Chemical Industries, *Sadhana*, 2000, **25**, p 519–559
3. U. Kamachi Mudali, R.K. Dayal, and J.B. Gnanamoorthy, Corrosion Studies on Materials of Construction for Spent Nuclear Fuel Reprocessing Plant Equipment, *J. Nucl. Mater.*, 1993, **203**, p 73–82
4. A. Ravi Shankar, V.R. Raju, M. Narayana Rao, U. Kamachi Mudali, H.S. Khatak, and B. Raj, Corrosion of Zircaloy-4 and its Welds in Nitric Acid Medium, *Corros. Sci.*, 2007, **9**(49), p 3527–3538
5. A. Ravi Shankar, R.K. Dayal, R. Balasubramaniam, V.R. Raju, R. Mythili, S. Saroja, M. Vijayalakshmi, and V.S. Raghunathan, Effect of Heat Treatment on the Corrosion Behaviour of Ti-5Ta-1.8Nb Alloy in Boiling Concentrated Nitric Acid, *J. Nucl. Mater.*, 2008, **2–3**(372), p 277–284
6. T. Karthikeyan, A. Dasgupta, S. Saroja, M. Vijayalakshmi, and V.S. Raghunathan, Studies on Weldability of Ti-5Ta-2Nb Alloy for Reprocessing Plant Applications, *Proceedings of the Conference on Materials and Technologies for Nuclear Fuel Cycle* (Covering Materials, Robotics, Process Instrumentation and Inspection Technologies), SERC, Chennai, Dec 15–16, 2003
7. Grant ken Hicken, Gas-Tungsten Arc Welding, *ASM Handbook*, Vol 6, Metals Park, OH, 1993
8. G.J. Guru Raja, Welding Titanium and Titanium Alloys—An Overview, *International Workshop on Recent Trends in Welding*, Bangalore, Oct 5–7, 1995
9. L.M. Gammon, R.D. Briggs, J.M. Packard, K.W. Batson, R. Boyer, and C.W. Domby, Metallography and Microstructures of Titanium and its Alloys, *ASM Handbook*, Vol 9, Metals Park, OH, p 899–917
10. J. Mathew Donachie Jr., *Titanium: A Technical Guide*, 2nd ed., ASM International, Metals Park, OH, 2000
11. W.A. Baeslack III, J.R. Davis, and C.E. Cross, Selection and Weldability of Conventional Titanium Alloys, *ASM Handbook*, Vol 6, Metals Park, OH, p 507–523
12. D.H. Phillips, Selection and Weldability of Advanced Titanium Base Alloys, *ASM Handbook*, Vol 6, Metals Park, OH, p 524–527
13. Corrosion of Non-Ferrous Alloy Weldments, *ASM Handbook*, Vol 13A, ASM international, Materials Park, OH, 2003, p 317–321
14. H.C. Dey, V. Shankar, C.R. Das, and A.K. Bhaduri, Weldability Study of Ti-Ta-Nb Alloy and Pure Ti, *Proceedings of the Conference on Materials and Technologies for Nuclear Fuel Cycle* (Covering Materials, Robotics, Process Instrumentation and Inspection Technologies), SERC, Chennai, Dec 15–16, 2003